PAPER Nr. : 98

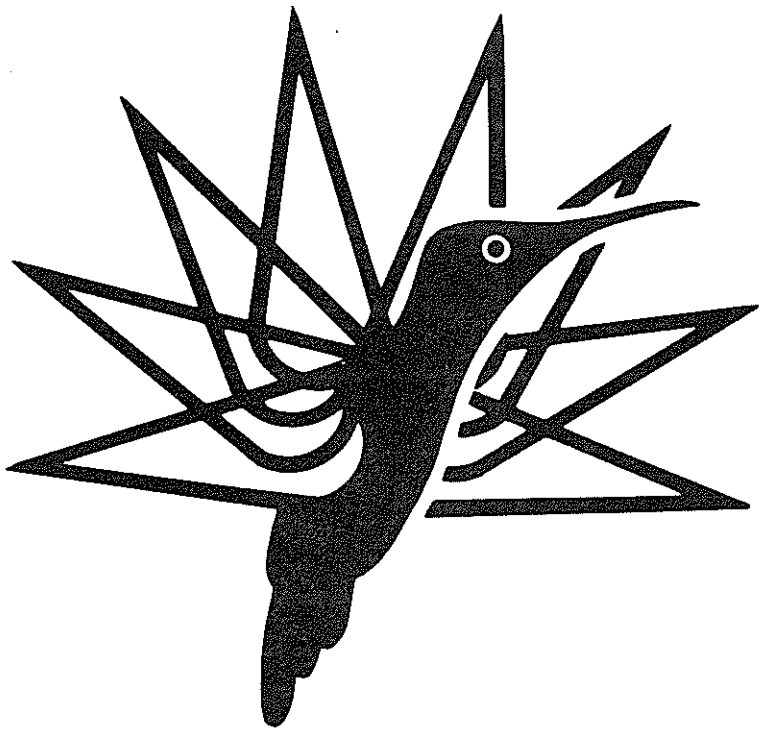

TESTS ON A NEW DYNAMICALLY SCALED MODEL ROTOR IN THE RAE 24FT WIND TUNNEL

BY

J. T. CANSDALE
R. J. MARSHALL
P. A. THOMPSON

ROYAL AIRCRAFT ESTABLISHMENT, FARNBOROUGH, ENGLAND

TENTH EUROPEAN ROTORCRAFT FORUM

AUGUST 28 – 31, 1984 – THE HAGUE, THE NETHERLANDS

TESTS ON A NEW DYNAMICALLY SCALED MODEL ROTOR IN THE RAE 24 FT WIND TUNNEL

by

J. T. Cansdale
R. J. Marshall
P. A. Thompson

Royal Aircraft Establishment, Farnborough, England.

ABSTRACT

A new dynamically scaled rotor has been developed for the RAE model rotor rig in the 24ft Wind Tunnel. Two trials have been conducted during 1983, with the aim of acquiring experimental data for validation of loads prediction methods and guiding their further development. Major features of the 3.6 m diameter rotor are the composite blades with RAE 9642 section and built-in twist, and the dual load path hub. The latter is readily adaptable to allow variation of basic design parameters.

The design and development of the rotor system is described, together with other new experimental equipment such as the data acquisition system. The trials are summarised, and a selection of results are presented covering loads measured in both the primary and secondary load path components. Comparable theoretical predictions are presented and discussed.

Plans for further developments of the test facility and the rotor itself are outlined.

1 INTRODUCTION

An accurate method of predicting loads in helicopter rotor blades and hub components is essential for the understanding of the behaviour of advanced rotor systems, and is vital in the design process. However, the calculation of these loads is a complex task, being dependent on both the aerodynamic flow around the rotor and the dynamic response of the rotor itself, and it is inevitable that any theoretical model will include some assumptions and empiricisms. The validity, or otherwise, of these must be checked by experiment, primarily by full scale flight trials or by model testing. The former is restricted by the availability and cost of hardware and by flight safety considerations; model testing, on the other hand, is not so constrained, and allows variation of many design and test parameters over ranges which would be unacceptable for flight test.

During the 1970's, a model test facility was developed for use in the 24ft Wind Tunnel at RAE Farnborough, with a view to obtaining systematic data specifically for the validation and further development of theoretical rotor analysis programs. The rig was described in detail in Ref 1, which also outlined some of the tests carried out on the original rotor, with its simple metal blades and hingeless (flexible element) hub. Much use was made subsequently of the test results, particularly by Westland Helicopters Ltd, for development of loads prediction methods (Ref 2).

With the increasing complexity of modern rotors, in respect of both the aerodynamic and structural design of blades and the advent of advanced hub configurations with multiple load paths, the task of load and performance prediction has become even more difficult, and there is once again a vital need for relevant experimental data. To this end, a completely new model rotor system has been built for the 24ft Tunnel test rig, featuring glass fibre reinforced plastic (gfrp) blades with a modern aerofoil section, in conjunction with a dual load path hub.

The paper describes the design and development of the new rotor and associated experimental systems, summarises the tests carried out and presents a selection of experimental results, with some analysis and comparisons with theoretical predictions. Plans are outlined for future model rotor test work.

2 MODEL ROTOR TEST STAND AND 24 FT TUNNEL

The test rig is shown in Fig 1, mounted in the 24ft Wind Tunnel; the schematic at Fig 2 gives an indication of the dimensions and positioning of the rotor, relative to the tunnel. The test stand, including the drive motors, gear box, control system and all components up to and including the swash plate are essentially as described by Anscombe[1]. The only major change is the new T-frame used to mount the tower on to the under-floor balance; this has overcome the drag problems encountered with the previous mounting. The tower is 4.5 m tall to support the rotor near the tunnel centre line and has a large mass of about 800 kg ensuring low natural frequencies and enabling it to withstand out-of-balance forces in the event of an accident. Between the tower and the T-frame are installed four elastomer blocks acting as compression springs, which lower the natural rocking frequency of the tower to 2 Hz so avoiding ground resonance problems with the new rotor at its normal operating speed of 600 rpm. The upper part of the tower is tiltable, and for all the tests to date has been set to 5° forward tilt to simulate forward flight. The main tower structure is enclosed in non-contacting, earthed fairings, reaching to within a few centimetres of the rotor, so that only rotor drag is transmitted to the balance.

The rotor drive is by four 15 HP motors, via an oil mist lubricated epicyclic gearbox. Three servo actuators control the collective and cyclic pitch settings at the swashplate. Instrumentation aspects are dealt with later.

The performance capabilities of the 24 ft tunnel itself should be noted. The maximum airflow speed attainable is approximately 40 m/s, the limitation being partly due to the torpedo netting used to protect the fan from the consequences of a model failure. The result of this is that either advance ratio or Mach number, but not both, can be made representative of full scale. In all the work to date, the tip speed has been chosen to give full advance ratio capability (up to 0.35), whilst accepting that this implies a Mach number roughly half that typical of full scale and hence an incorrect simulation of compressibility effects. This limitation is acceptable however for tests in which the aim is the substantiation of computer programs primarily concerned with predicting the dynamic behaviour of rotors.

3 ROTOR SYSTEM

3.1 Overall design philosophy

The limitations imposed by the tunnel influenced the design of the new rotor, and resulted in near Froude scaling. The aim was to achieve a model, roughly one quarter of full size, having correctly scaled dynamic characteristics, particularly in respect of the placing of the lower order vibration modes relative to the rotational speed. It was not however intended to build a scale representation of any particular full scale rotor, although data from both the Lynx helicopter and the WHL WG34 (Sea King Replacement) design study were used for guidance. One major factor was that the model rig was configured for three bladed rotors; in designing the new model, the blade chord was increased proportionally to give a solidity equal to that of Lynx. This increase had subsidiary benefits in facilitating the blade manufacture and the fitment of instrumentation, but made exact scaling of both loads and vibration modes impossible. Thus, the net result of the various design compromises is a rotor which is dynamically representative of typical modern rotors, whilst not accurately scaling any particular one.

The major features of the rotor are as follows:

Rotor diameter:	3.6 m
Number of blades:	3
Blade chord:	140 mm
Solidity:	0.0743
Rotational speed (nominal):	600 rpm
Tip speed (hover):	113 m/s
Aerofoil section:	RAE 9642
Built-in twist:	4.4°/m, nose down towards tip
Effective hub offset:	14%

3.2 Blades

As stated above, the structural properties of the blades were originally based on Lynx, with subsequent adjustment to suit the proposed WG34 design. The only major deviation from dynamic scaling was in respect of the torsional stiffness which was chosen to be significantly higher than the true scale value, thus limiting the aeroelastic response of the blade. This was done mainly to create a docile rotor for the initial studies which were aimed at generating a data base prior to future investigations of more ambitious rotors with unconventional planforms and/or dynamic characteristics (e.g. aeroelastically tailored rotors). In practice, this decision also eased the blade design and manufacture. The effect on the torsional response was to place the first torsional mode at just below 9/rev (at the standard rotor speed of 600 rpm), roughly twice that typical of full scale. The full modal analysis of the rotor is presented later (Section 3.4).

The basic blade construction comprised a glass fibre/epoxy composite D-spar, with a balsa trailing edge, as shown in Fig 3. A number of candidate designs were considered, both by theoretical calculation of section characteristics and by manufacture and testing of specimens. After some preliminary efforts with cold cure resins, which proved to have unacceptable creep and hysteresis properties, hot cured systems were used, with the components being cured in light alloy moulds. The D-spar is made initially in three components, namely the main "C", a small doubling insert at the leading

edge, and the channel section to close the "D". All are made from unidirectional,preimpregnated glass cloth, 0.127 mm thick, with the angles of the plies adjusted in the lay-up to give the required values of flap, lag and torsional stiffnesses, and to place the chordwise location of the shear centre. The blade is completed by the leading edge weight, the instrumentation looms, the glass-cloth skinned balsa trailing edge fairing, the tip weight and the tip fairing.

3.3 Hub

At the time that the design commitment was made on the new rotor, great interest was being shown in the use of dual load path hubs (similar in principle to the Aerospatiale Starflex system), this type being favoured for the WG34 design. It is of particular interest to test such a hub, since the theoretical modelling of the dual load paths imposes problems not encountered with either articulated or semi-rigid hubs. A further aim with the model hub was to achieve versatility, with the ability to vary easily the physical parameters of the hub (geometry, stiffnesses,etc).

Schematic views of the hub are shown in Figs 4, 5 and 6, showing respectively the primary load path components, carring the centrifugal and pitch control loads (Fig 4), the secondary load components, providing stiffness in flap and restraint with damping in lag (Fig 5), and the assembled system (Fig 6). Fig 7 shows the actual hardware.

Notable features of the hub include:

-the use of a spherical elastomeric bearing in the primary load path to carry the centrifugal loads whilst allowing freedom in flap, lag and pitch;

-the flap flexures (Fig 5), which govern the stiffness in the flapping plane and determine the rotor control power;

-the elastomeric blocks providing both stiffness and damping in lag, and hence setting the first lagwise modal frequency;

-the swept links. Sets of links with different stiffnesses and sweep angles were used. One set also featured postcone, i.e. a flapwise change of angle at the joint between the link and the blade;

-adjustable precone, achieved by interchangeable wedge blocks at the flap flexure mounting.

3.4 Overall rotor characteristics

Throughout the development of the rotor, extensive use was made of all available theoretical design programs to predict the loading and preformance characteristics , supported by laboratory measurements of physical properties. Fig 8 shows the calculated vibration modes for the complete rotor, based on the best available input data. It will be seen that at the normal rotational speed of 600 rpm, none of the lower order modes coincides with an exact multiple of rotor frequency. Further, the lower modes are separated from one another, thereby minimising dynamic coupling effects. The combination of a fundamental test tower frequency of 2.2 Hz with the first lag mode at 6 Hz removes the possibility of ground resonance at 600 rpm. However in running up to 600 rpm, the rotor passes through a potential ground resonance at 480 rpm,

but the damping provided by the damper pads precludes any build-up of vibration. Thus for the first tests with the new rotor system, all reasonable precautions were taken to avoid low frequency dynamic problems.

One factor revealed by the loads analysis was that the full range of rotor thrusts, from zero up to the onset of stall, could not be covered by a single precone configuration, the limitation being imposed by loads in the flap flexures and swept links. Precone settings of 3° and 5° were therefore used for the lower and upper thrust ranges respectively.

4 INSTRUMENTATION

4.1 Rotor loads and other experimental parameters

Strain gauge bridges are used on the blades and hub components to measure loads and moments, as shown in Fig 9. In the majority of the positions, flapwise, lagwise and torsional moments are measured. On the flap flexures, the strain gauges are calibrated to measure the flapwise and lagwise forces; there should be no transfer of torsional loads from the primary to the secondary systems via the coupling bearing. Pitch link loads are also monitored.

At present, no total loads/moments balance is fitted to the model, although a system is planned for the future (see Section 7.1). The prime purpose of the current experiments is adequately served by the measurement of loads in the individual components, as given by the strain gauges.

Overall lift and drag on the rotor are measured by the tunnel balance. Other parameters measured include rotor speed, shaft torque and collective/cyclic pitch.

4.2 Data acquisition system

The data acquisition system is shown schematically in Fig 10. Strain gauge signals from the rotating components are taken to a 45-channel amplifier system mounted on the hub, and thence via slip rings to safety monitoring displays and to the main 64-channel data processing and recording system; other signals from the non-rotating components are also input at this point. Further gain and offsets are applied, as necessary, to each channel, after which the signals pass through filters to sample-and-hold circuits which enable all 64 channels to be sampled simultaneously; thus all measurements on the rotating system are made at a common azimuth position. The data are then multiplexed, digitised and written to an external memory. The Hewlett-Packard 1000E Series on-line computer transfers the data from memory to its own store, takes an average from a specified number of revolutions (normally 16), and finally writes the data to disc. The averaging is needed to smooth the effects of tunnel turbulence.

The data are processed post-run,again using the HP computer. Firstly a fast Fourier transform is applied to correct for the phase errors introduced by the electronic packages. The data are then converted back to the time domain and the calibration factors applied to yield load and moment values. Finally, the data are written to magnetic tape and transferred to a VAX computer for analysis and comparison with theory using the DATAMAP suite of computer programs (Ref 3).

5 EXPERIMENTS

Two series of tests were conducted on the new rotor system during 1983. The primary aims of the first were as follows.

a. To confirm the predicted safe flight envelope for the new rotor, as defined by allowable steady and oscillatory loads in critical components such as the flap flexures and swept links.

b. To prove all the new components of the rotor, test rig and data acquisition system.

c. To lay down a set of results, covering a range of test conditions and rotor configurations, for immediate use in validation of loads prediction programs and as a datum for future reference and comparison with more complex rotors.

The tests covered thrusts of 300, 450 and 600 N (equivalent to C_T/σ values of 0.0255, 0.0383, 0.051) with 3° precone, and 600, 750 and 900 N (C_T/σ =0.051, 0.0638, 0.0765) at 5° precone. At each condition, the advance ratio (μ) was varied from 0.1 to 0.34 in increments of 0.02. Swept links with 5° sweep angle were used throughout. At each test point, thrust, drag and all hub and blade loads were recorded. These tests were then repeated with a stiffer set of swept links, again with 5° sweep.

As a result of these tests, several modifications were made to the hub. Steady lagwise loads in the flap flexures were lower than expected, whilst those in the swept links proved to be higher; further calculations showed that a change from 5° to 2° sweep angle would produce a better compromise between the loads in these two components. A further modification involved simplification and lightening of the lag damper coupling bearing assembly.

In the second series, the tests once again covered a range of thrust and advance ratios. Primary objectives were as follows.

a. To acquire a comprehensive set of loads and performance data for the modified rotor (2° sweep and new coupling bearing).

b. To acquire data at a range of rotor speeds from 300 to 600 rpm.

c. To investigate the effect on rotor loads of three shapes of fairing being considered as candidates for a planned new rotor-head data processing system (see 7.1 below).

d. To examine the effect of trimming the rotor to give zero 1/rev flatwise bending moment in the swept links, rather than in the flap flexures, as done previously. The rotor loads program allows two options for trimming, namely

(i) a bending moment trim, which produces a specified first harmonic flap moment at the trim station, and

(ii) an secondary load path force trim, which produces a specified first harmonic flap force in the secondary load path.

Initial predictions from the program suggested a difference in the loads distribution depending on the option chosen, whereas the experiments showed no difference. This discrepancy was finally removed by two changes to the

analysis. Firstly, modifications were made to the program to allow for centrifugal loads on the SLP components (lag elastomer housing, flap flexures, etc); and secondly, it was found that elimination of the 7th mode (4th flap, see Fig 8) from the analysis removed any remaining differences. The justification for the latter is discussed fully in Ref 4.

6 RESULTS AND ANALYSIS

6.1

The results presented fall into two groups. Firstly, Figs 11 to 19 show a selection from the original datum tests with the rotor running at 600 rpm, and include corresponding theoretical predictions for comparison. Secondly, Figs 20 to 23 show results taken from the study of loads variation as a function of rotor speed. In both cases, loads in both primary and secondary load paths are given.

Before discussing the results in detail, it is useful to summarise the loads prediction technique itself. The method, which is described fully in Ref 5, involves the calculation of the blade and hub modal characteristics, followed by the solution of the forced response equations. For the modal calculations, the secondary load paths are represented by point linear springs for the flap and lag restraint (applied at the appropriate point on the tension member) and by a linear spring on the end of a weightless arm for the control system.The mass of the coupling bearing assembly is included in the overall mass distribution of the primary structure, i.e. as a mass on the tension member. Precone, postcone and sweep are represented by the locus of the shear centre. For the aerodynamics, the vortex ring wake model of Ref 5 is used; this includes an interactive near wake and models of the dynamic stall process.

Throughout the analysis of the results, the primary concern has been with oscillatory, rather than steady loads, giving particular attention to the amplitude and phasing of the harmonic contributions, since it is these that are most dependent on the accurate modelling of the dynamic characteristics and aerodynamic forcing. In general, the steady components were well predicted by theory.

6.2 Datum tests

Considering first the primary load path, Figs 11 to 13 show flatwise bending moments on the blade. At low advance ratio and high thrust (Fig 11) the agreement is very good. However, with increasing advance ratio, the theory tends to overestimate the 3/rev component, leading to the poorer correlation seen in Fig 12. At low thrust and high advance ratio, with 3° precone (Fig 13) the agreement is rather better. Similar trends were seen for all three blade stations and for flatwise moments in the swept links. Overall, the correlations were fairly reasonable except for the general tendancy for overestimation of the 3/rev as thrust and μ were increased.

Typical edgewise moments are shown in Figs 14 and 15. In general, the theory underestimates the peak to peak magnitude of the 1/rev component in both the blades and the primary hub components. Also, as the advance ratio increases, the calculated loads tend towards a pure 1/rev oscillation, with decreasing higher harmonic content, whilst the test results retain the higher harmonics. The sources of this disagreement are difficult to isolate since

edgewise loads (particularly the first harmonic) may originate either directly from aerodynamic forces or from Coriolis forces due to blade flapping. Further tests with more extensive instrumentation to measure flapping motions and blade loads at more blade stations will help to clarify this.

The torsional moment in the swept link is shown in Fig 16, and is typical of results for all points in the primary system. In general, the first harmonic is fairly well predicted, but the higher harmonics, giving the flattening of the peaks and troughs, are lacking. As would be expected, the pitch link loads (Fig 17) show a similar character to that of the torsion moment, with an overprediction of the first harmonic and a notable absence from the calculations of the higher harmonics.

Regarding the secondary load path components, the predictions of flapping force in the flapping flexures (Fig 18) have the correct basic form, but for the most part overpredict lower harmonics. The lagwise forces measured experimentally are dominated by a higher harmonic component (Fig 19) which in this case is the tenth harmonic. Further test evidence has shown the absolute frequency of this to be remarkably independent of rotor speed, appearing to originate from a natural resonance at about 97 Hz, which is forced to the nearest harmonic. This is discussed below in Section 6.3.

Overall the comparisons between experiment and theory appear better on the blades than on the hub elements, although there is room for improvement on both. It is notable that similar comparisons for flight tests on a Puma helicopter (Ref 5) showed a generally better correlation, albeit for a rotor of conventional design. For the present results, the preliminary analysis has not pinpointed any particular deficiencies of the theoretical model as the cause of the discrepancies; however further analysis, together with results from future tests,should identify the principal sources of error. Of particular help will be the testing of a more heavily instrumented rotor which will allow use of the SPA (strain pattern analysis) technique developed at RAE (Ref 6) for derivation of mode shapes and frequencies for the rotating blade. Efforts will also be made to confirm and improve the quality of the physical input data (stiffnesses, inertia, etc) for the model rotor.

6.3 Study of rotor speed

The results in Figs 20 to 23 show the effect of rotor speed on the flapwise and lagwise forces in the flap flexures and the edgewise and torsional moments in the blades.

In Fig 20, the flapwise load is dominated by the 2/rev, with little variation of phasing with speed. However at 500 rpm, a strong 3/rev component is apparent, corresponding to the second flap mode which is almost exactly coincident at this speed (see Fig 8). At 300 rpm, the second flap mode is beginning to appear as 4/rev.

In Fig 21, the form of the edgewise moments on the blade is consistent for 600, 500 and 400 rpm, with little change of phasing or amplitude. However, as the speed drops to 300 rpm, close to the coincidence of the first lag mode with 1/rev, the phasing alters radically, with a shift on first harmonic of some 85°.

The torsional moments shown in Fig 22 have a dominant first harmonic, with little phase change, as would be expected with the torsionally stiff system. The peak-to-peak amplitude is almost exactly proportional to the square of rotor speed.

Fig 23 again shows the unexplained higher harmonic seen in Fig 19. The frequencies are respectively 19, 15, 12 and 10/rev at 300, 400, 500 and 600 rpm, suggesting a natural mode at 97 Hz being forced to the nearest harmonic. At present its origins are unknown, although one possibility to be considered is a collective lagwise mode caused by the flexibility of the transmission, etc (which is not included in the theoretical model). Further investigations are planned.

7 FUTURE PLANS

Future activities fall into two categories, namely those to extend the testing capabilities, by modifications to the existing rig or by acquisition of new test rigs, and the actual programme of experimental work on the dynamics and aerodynamics of new rotor systems.

7.1 Rig modifications

Three major improvements to the 24ft Tunnel rig are planned.

i) The hub is to be modified, with replacement of the flap flexures by a pivotting frame, still providing lagwise restraint via the lag elastomers, but being freely articulated in flap. The option of using the flap flexures will also be retained. At present, the flapping loads in the flexures represent one of the major limitations to the rotor operating envelope (e.g. requiring use of two precone settings to cover the full thrust range). The aim of the articulated hub is to remove this constraint for forthcoming work on more complex (and hence less predictable) rotors, where unexpectedly high loads may be encountered.

ii) A piezo electric balance system is to be incorporated into the hub, between the shaft and the main spool, for measurement of six components of loads and moments. This will enable studies to be made on the sources and alleviation of vibratory loads.

iii) A further stage in the development of the data acquisition system is proposed, with incorporation of amplifiers, filters and sample/hold units into a hub mounted package. This will enable digitised, multiplexed signals to be taken down the slip rings, so that a larger number of parameters may be measured in the rotating system. (The rig design prohibits any increase in the number of slip rings.)

7.2 5m Tunnel rig

Project definition studies are under way for a completely new test rig for use in the RAE 5m Wind Tunnel. The working section of 5 m x 4.2 m, the speed capability of over 90 m/s and the high quality of the flow make this tunnel ideal for model rotor studies and will allow use of correct Mach scaling. The proposed rig will accomodate rotors of up to 3 m diameter, with a drive system of approximately 120 kW. It will be used for dynamics investigations, with a particular interest in aeroelastically tailored rotors, together with further aerodynamic studies.

7.3 Future test programme

The thorough study of the current rotor will be continued, including full analysis of the two 1983 trials and some further testing this year; this will include use of the SPA blade (Ref 6) together with various laboratory investigations of modal behaviour and other aspects to quantify better the physical characteristics of the rotor. Once these efforts have led to confidence in a full understanding of the datum rotor, progress will be made to more complex designs. As a first step, a more torsionally soft blade will be run later this year, having a first torsional mode more representative of current full scale practice (i.e. around 5/rev).

Subsequent plans include (a) studies of the use of mass distribution changes , both chordwise and spanwise, to tune modal shapes and frequencies and introduce couplings; (b) use of a swept tip in conjunction with the torsionally soft blade to force the torsional response of the blade; and (c) studies of more structurally complex blades, with deliberate couplings introduced by use of asymetric constructions or fibre lay-ups. The last will be done as a series of parametric studies to provide guidelines in the use of aeroelastic tailoring for vibration alleviation and performance enhancement.

8 CONCLUSIONS

The new rotor system has been thoroughly tested and shown to be a safe and versatile tool for studies of rotor dynamics. Other new features of the rig, such as the data aquisition system, have also been well proven.

The tests to date have yielded a substantial data base for the basic rotor. Initial comparisons of the data with theoretical predictions are encouraging, although they are not as good as previous correlations for an articulated rotor and leave a number of unresolved questions. Further analysis, together with the planned programme of tests with more extensively instrumented blades (e.g. the SPA blade), is needed to clarify the origins of the discrepancies, and thus arrive at a full understanding of the datum rotor. This is a necessary step before progressing to more complex designs for which there is less confidence in the prediction methods.

The proposed long term programme of rig improvements and experimental investigations will make a considerable contribution to the understanding of the dynamics of complex rotor systems and the refinement of loads prediction methods. In particular it will provide the basis for the application of aeroelastic tailoring for performance enhancement and vibration reduction.

REFERENCES

1 Anscombe, A; Cox, A P; Marshall, R J: Wind tunnel testing of model rotors at RAE Farnborough. Paper 34, Second European Rotorcraft and Powered Lift Forum, 1976.

2 Hansford, R E. The comparison of predicted and experimental rotor loads to evaluate flap-lag coupling with blade pitch. Paper 19, 34th AHS Symposium, 1978.

3 Philbrick, R B. The data from aeromechanics test and analytics - management and analysis package (DATAMAP). USAAVRADCOM TR-80-D-30, 1980

4 Thompson, P A. A comparison of predicted and measured loads on a split load path rotor. RAE Technical Report TR 84057, 1984.

5 Young, C. Prediction of aerodynamic loads on rotorcraft. Paper 11, AGARD-CP-334, 1982.

6 Walker, A R. Further application and development of strain pattern analysis. Paper 7.2, Eighth European Rotorcraft Forum, 1982.

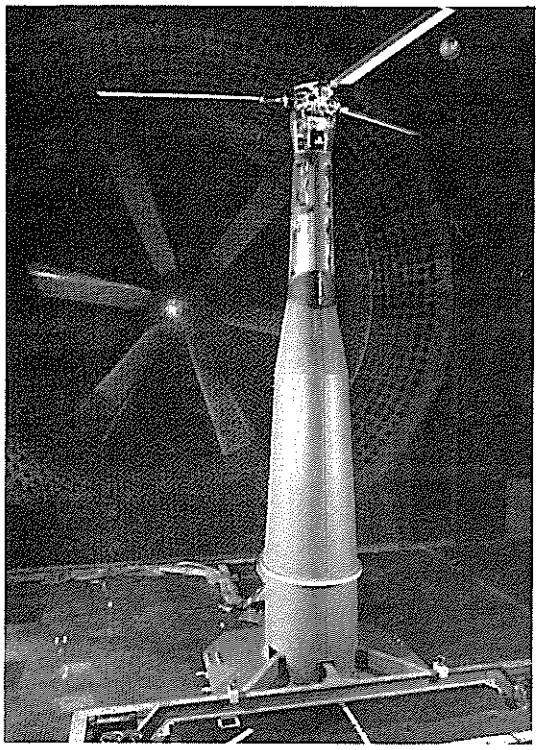

Fig 1 Model rotor rig in RAE 24ft wind tunnel

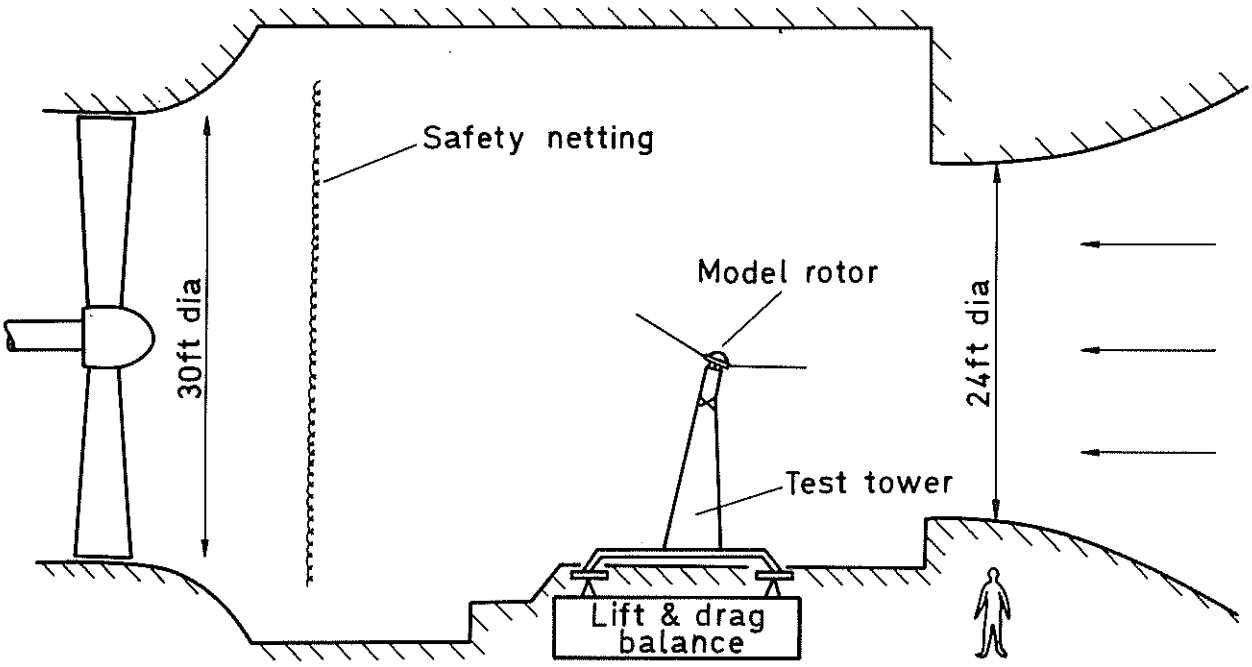

Fig 2 Schematic layout of model rotor rig in RAE 24ft wind tunnel

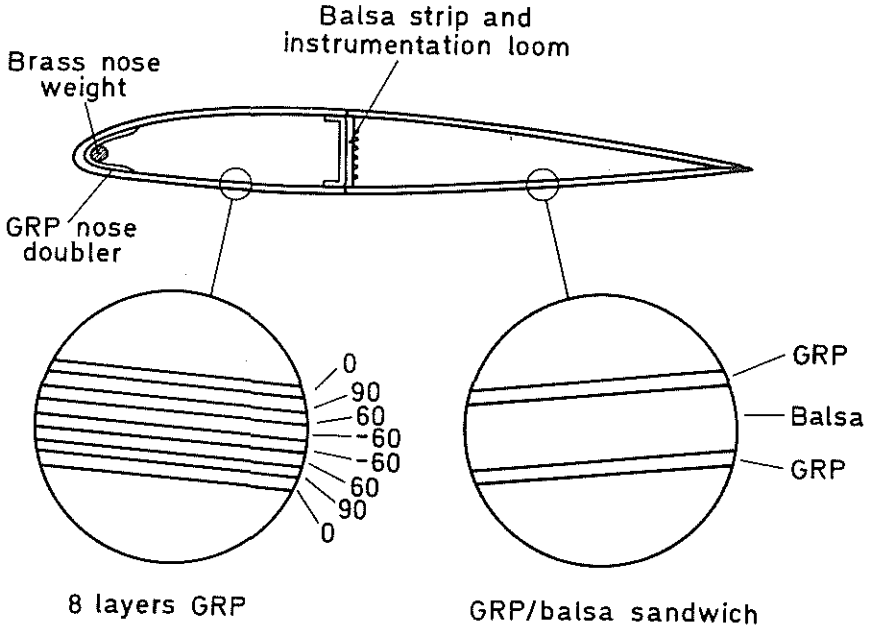

Fig 3 Blade construction

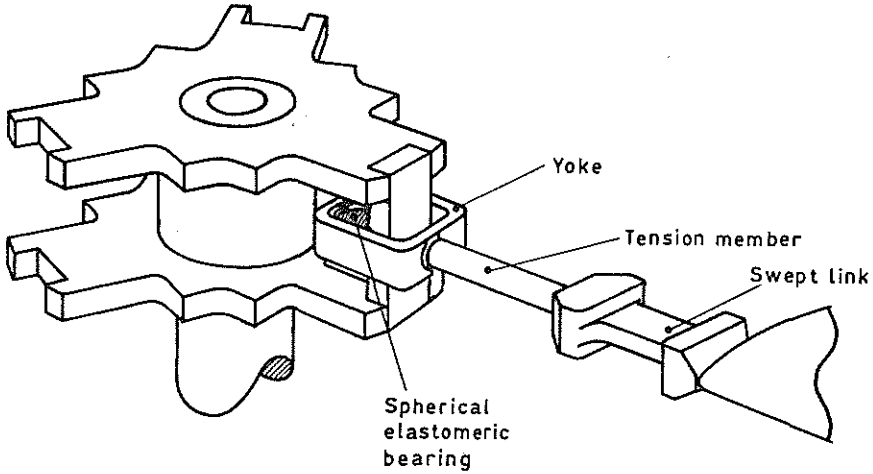

Fig 4 Hub assembly — centrifugal load carrying elements

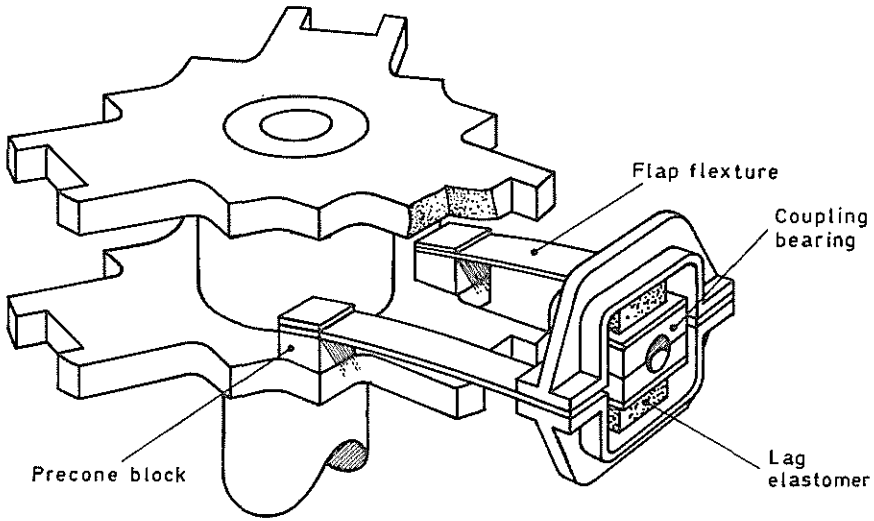

Fig 5 Hub assembly — flap and lag flexural elements

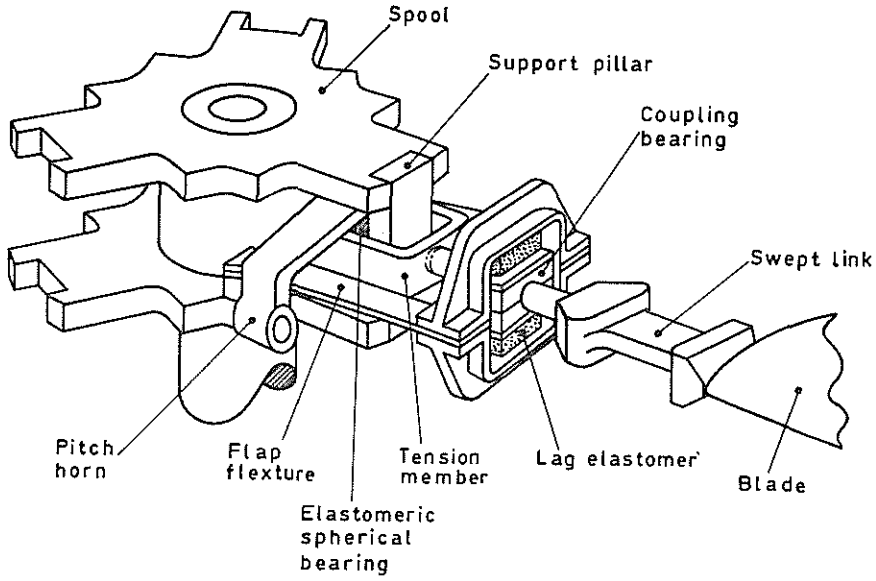

Fig 6 Complete hub assembly

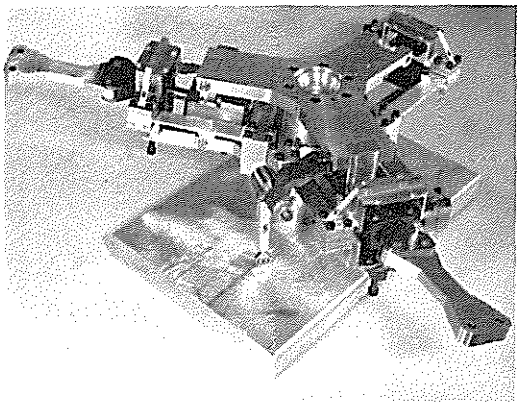

Fig 7 Complete hub

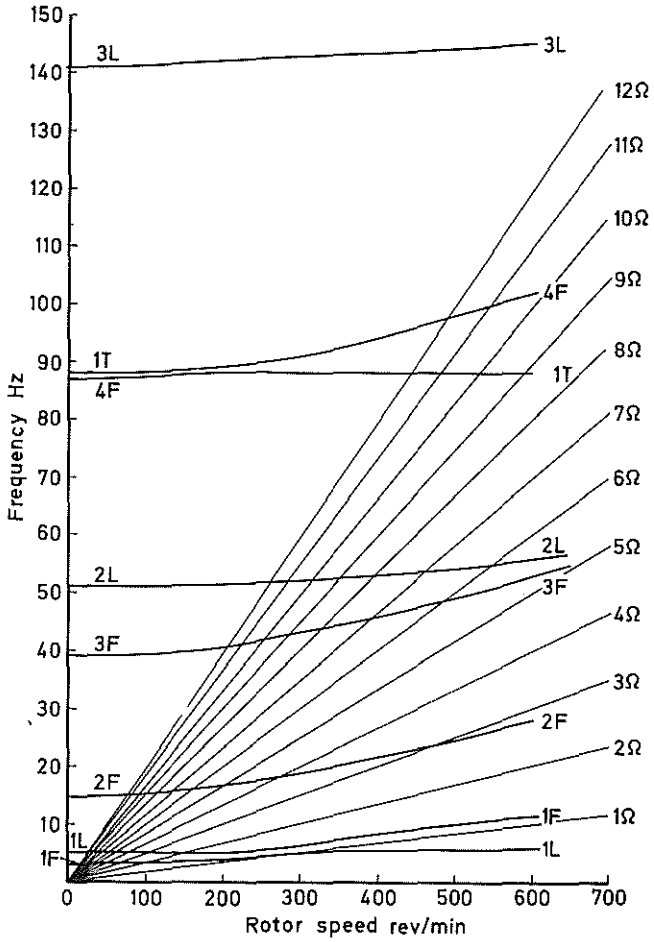

Fig 8 Modal characteristics of rotor system

⊠ Strain gauging for flatwise , edgewise & torsional moments

□ Strain gauging for flap and lagwise loads

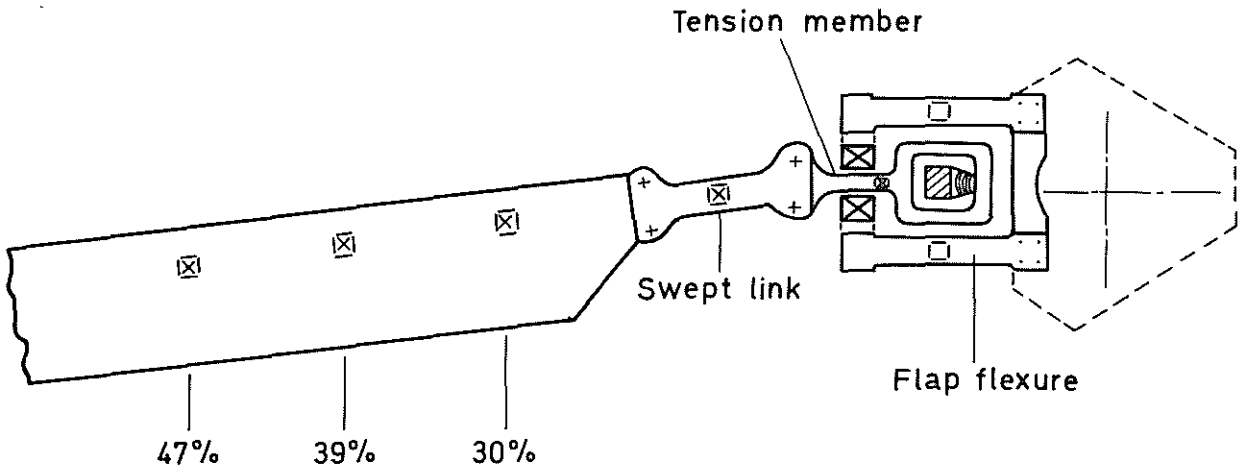

Fig 9 Strain gauging of blade 1 and hub

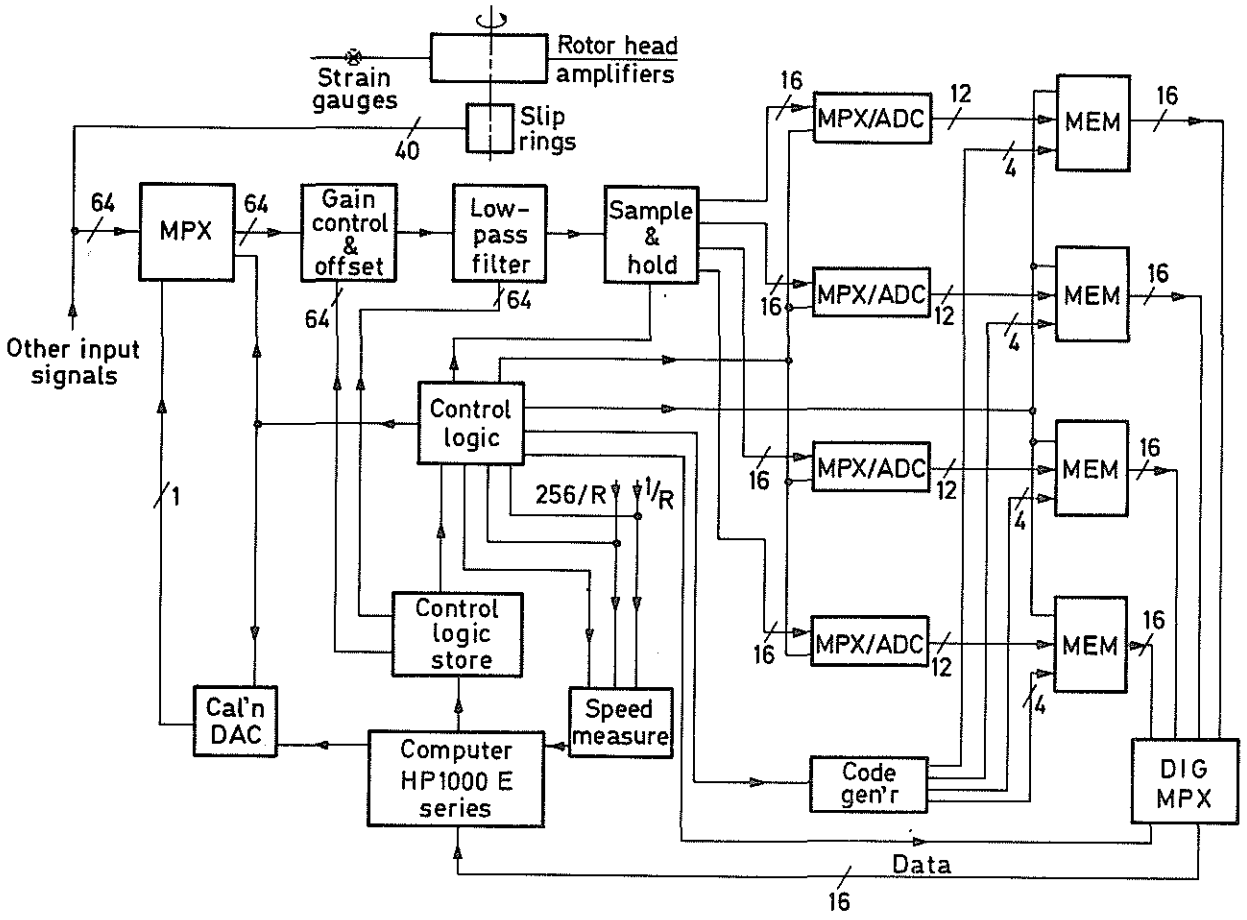

Fig 10 Block diagram of data acquisition system

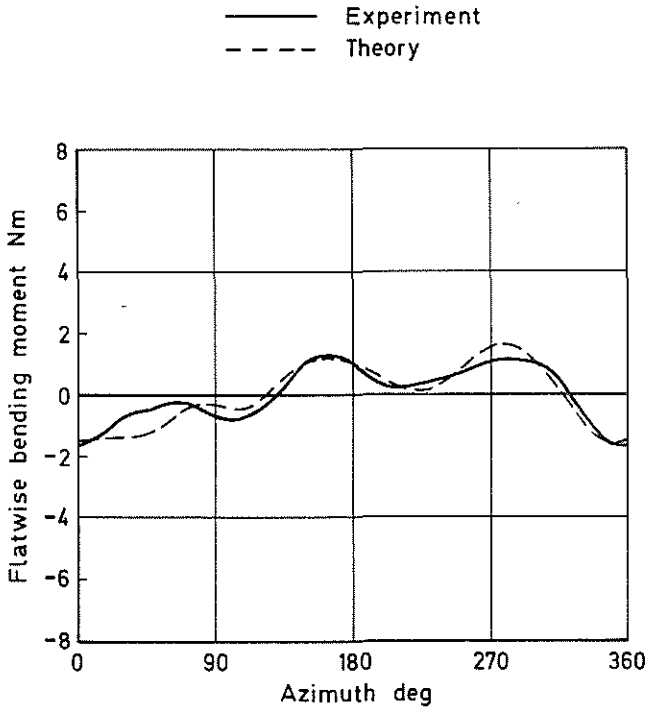

Fig 11 Flatwise bending moment on blade at 39%R. μ = 0.1, T = 900N, C_T/σ = 0.0765

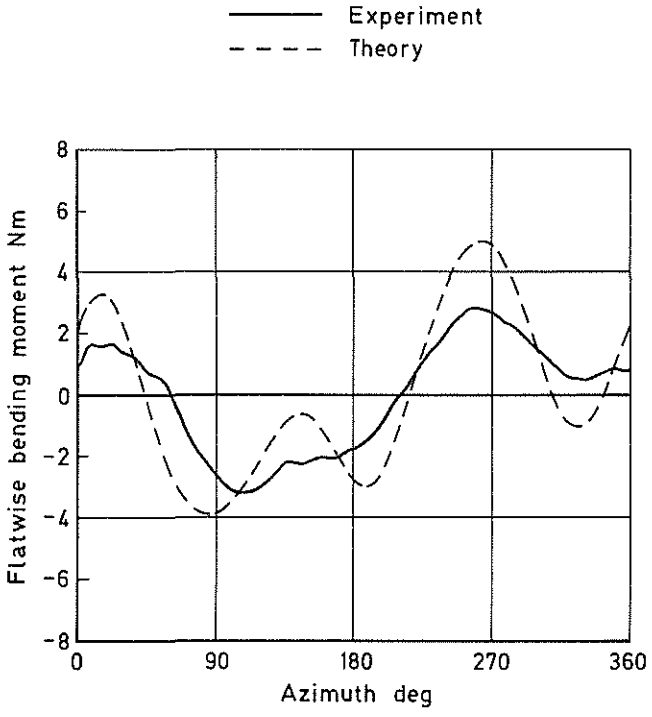

Fig 12 Flatwise bending moment on blade at 39%R. μ = 0.34, T = 900N, C_T/σ = 0.0765

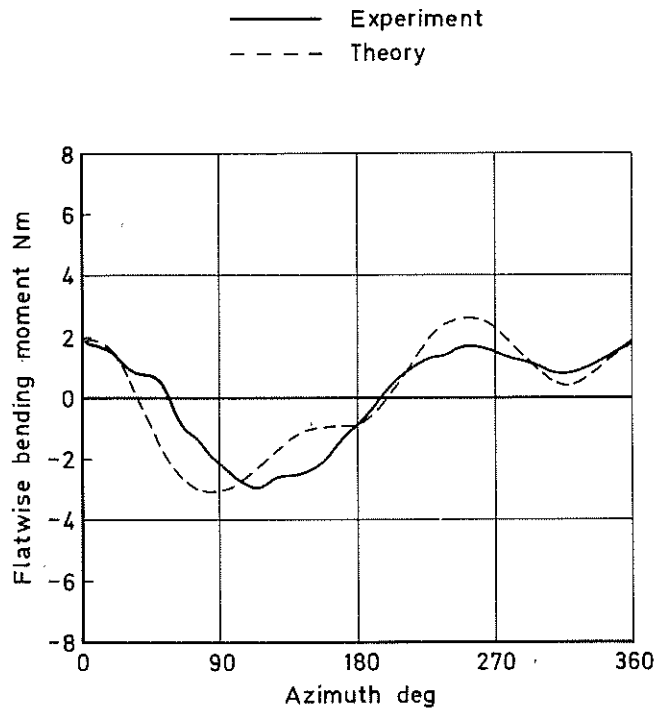

Fig 13 Flatwise bending moment on blade at 39%R.
μ = 0.34, T = 300N, C_T/σ = 0.0255

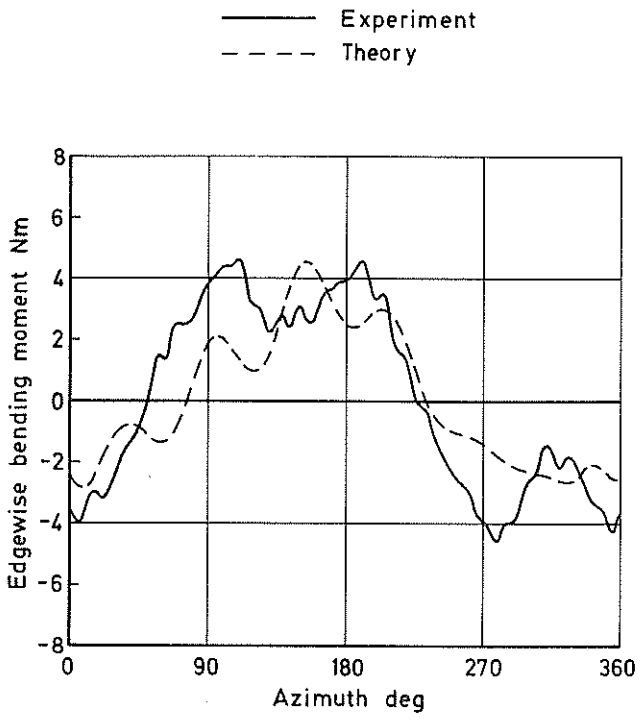

Fig 14 Edgewise bending moment on blade at 39%R.
μ = 0.2, T = 900N, C_T/σ = 0.0765

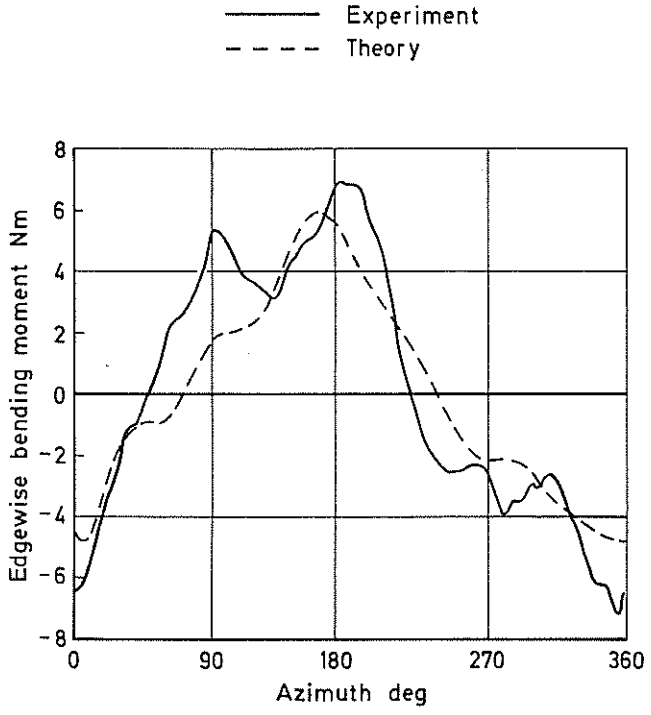

Fig 15 Edgewise bending moment in blade at 39%R.
μ = 0.34, T = 900N, C_T/σ = 0.0765

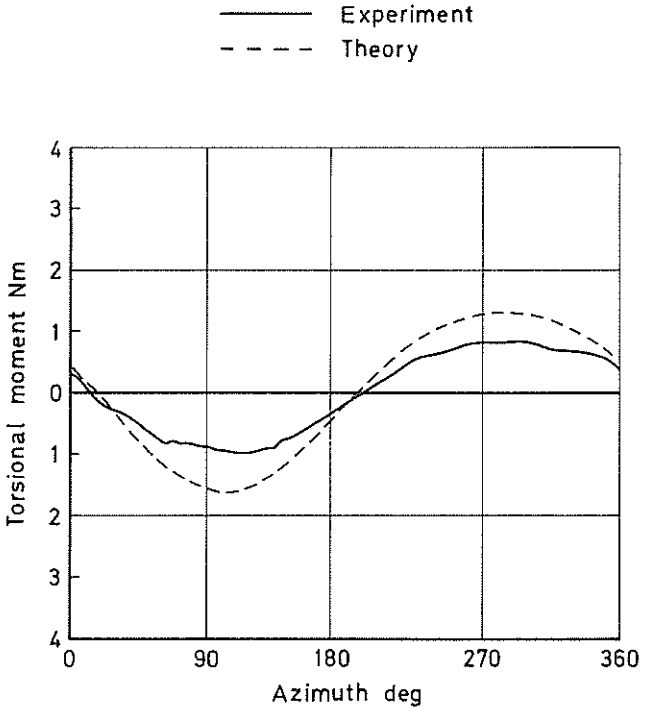

Fig 16 Torsional moment in swept link.
μ = 0.2, T = 300N, C_T/σ = 0.0255

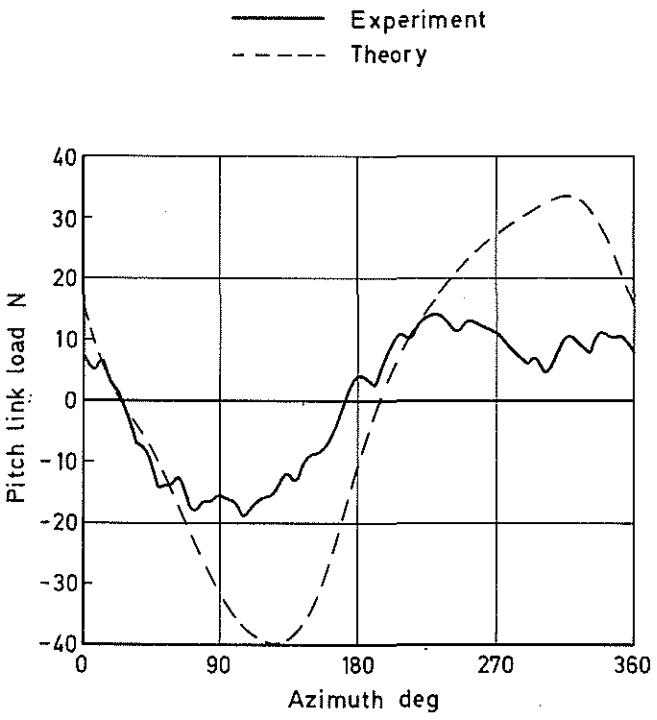

Fig 17 Pitch link load.
μ = 0.34, T = 900N, C_T/σ = 0.0765

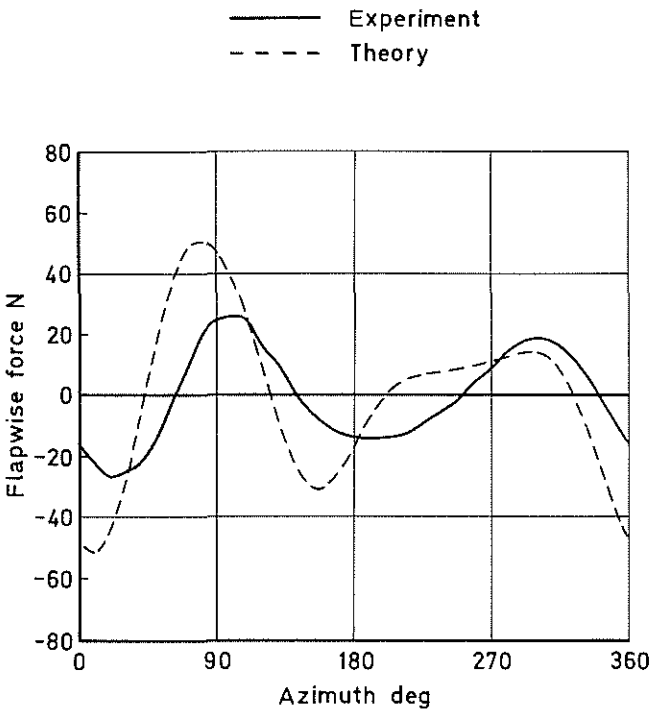

Fig 18 Flapwise force in flap flexures.
μ = 0.34, T = 750N, C_T/σ = 0.0638

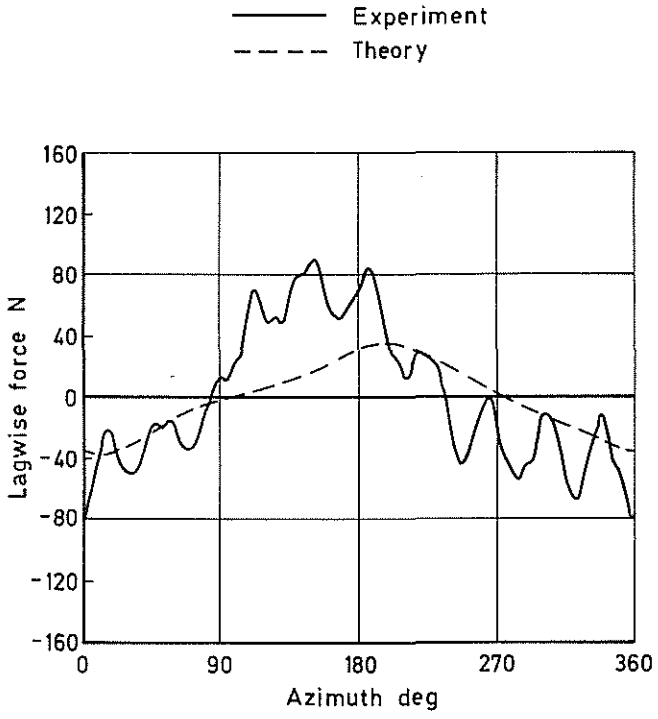

Fig 19 Lagwise force in flap flexures.
μ = 0.34, T = 600N, C_T/σ = 0.051

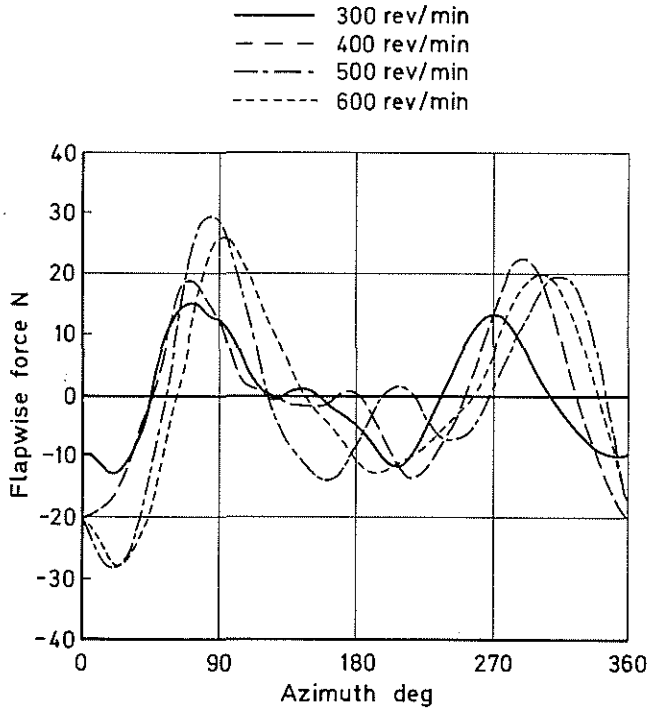

Fig 20 Variation of flapwise force in flap flexures with rotor speed. μ = 0.34, C_T/σ = 0.051

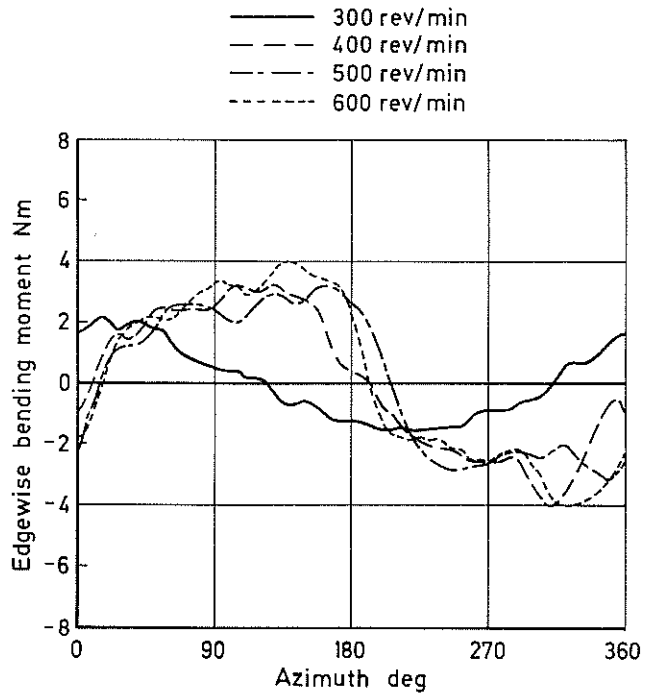

Fig 21 Variation of edgewise bending moment on blade at 31%R with rotor speed $\mu = 0.34$, $C_T/\sigma = 0.051$

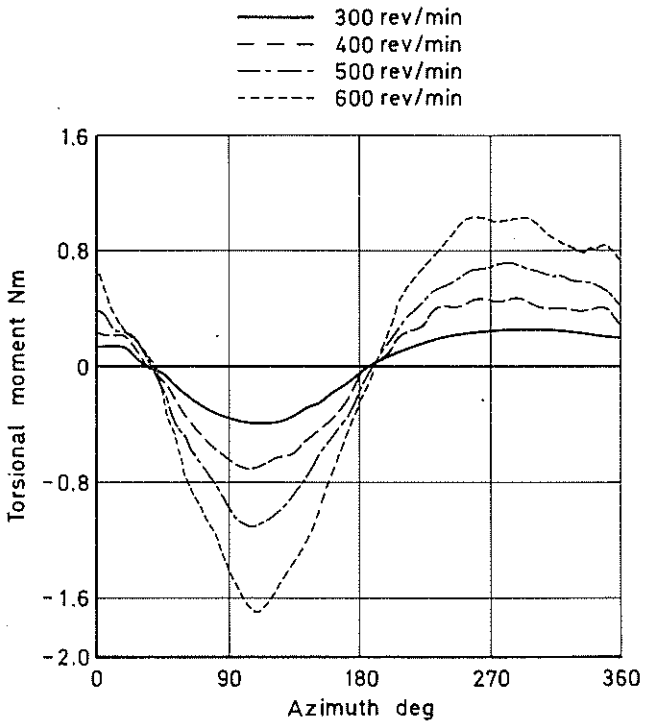

Fig 22 Variation of torsional moment in blade at 31%R with rotor speed. $\mu = 0.34$, $C_T/\sigma = 0.051$

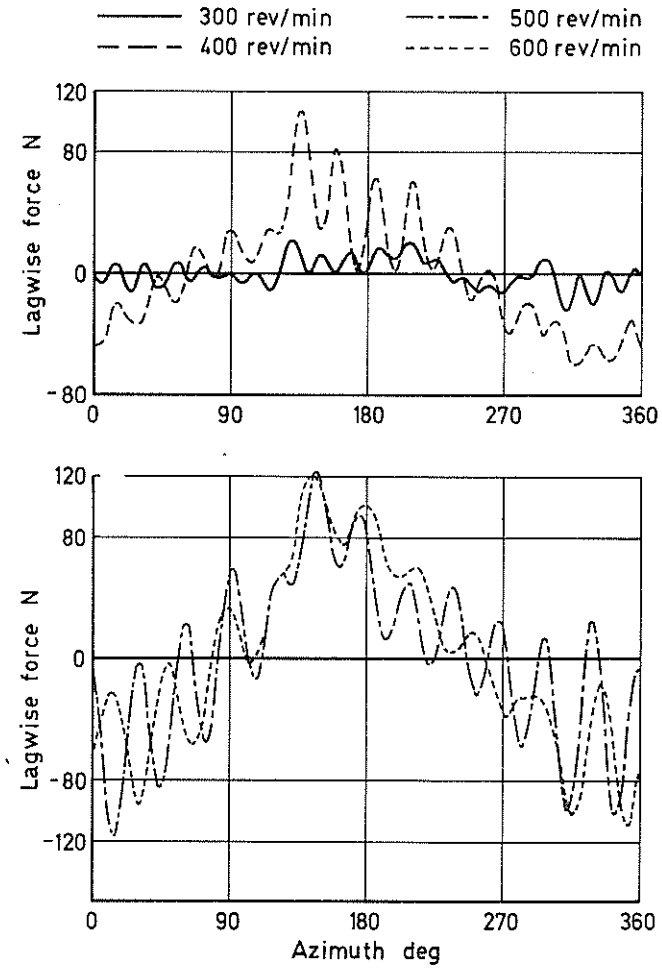

Fig 23 Variation of lagwise force in flap flexures with rotor speed. $\mu = 0.34$, $C_T/\sigma = 0.051$